Study of a transport barrier in GOLEM with probes

David Vaquero Cerezo[1, 2] and Yashpreet Sehmbi[1, 3]

[1]Master of Science in Nuclear Fusion and engineering physics
[2]University of Stuttgart, Pfaffenwaldring, 70569, Stuttgart, Germany
[3]Institute of Plasma Physics of the CAS, Za Slovankou 3, 182 00 Prague 8, Czech Republic

***Abstract*—Expanding on the work [5] done on the observation of spontaneous formation of transport barrier in a helium plasma in a circular tokamak, we present an improved study featuring a new and improved experimental dataset and data analysis methodologies. Based on the combination of old and new data, new scaling laws are derived, which highlight the dependencies of the transport barrier formation on key plasma parameters. The measurements were made using a combined ball-pen and Langmuir probe assembly on a shot-by-shot basis. The scaling laws pave the way for possible reproducibility of the transport barrier in other tokamaks with circular cross-section, reigniting interest in them for fusion-relevant studies.**

I. Introduction

Transport barriers are localized regions within the tokamak plasma, where the turbulence-driven transport of particles, heat, and/or momentum is significantly reduced, playing a crucial role in enhancing plasma confinement and improving the performance of fusion devices. The formation of transport barriers has been observed in various tokamaks like ASDEX, DIII-D, JET, and COMPASS, for example during H-mode, which involves barrier in both electron temperature and density when the power input exceeds a certain threshold. While spontaneous formation has been achieved in divertor configurations, limiter configurations have required the use of a biasing electrode to polarize the plasma, which is impractical for tokamak operation. However, a recent experiment on a circular plasma in the GOLEM tokamak in helium plasmas has demonstrated the spontaneous formation of a transport barrier, characterized by a steep gradient of electron temperature in the scrape-off layer, accompanied by an increased electric field, offering a relevant method for studying transport barriers in tokamaks with circular cross-section.

The previous study [5] investigated how the formation of the transport barrier depends on both plasma density and current, but found that input power was the primary factor affecting the transport barrier, with no conclusive results suggesting dependence on plasma density. The current study extends this work by keeping plasma density and magnetic field constant while varying plasma current, which is controlled by the voltage on the current discharge capacitor.

During the data analysis phase, new data from the current scans was combined with the existing database from the SUMTRAIC study to examine the relationship between plasma density and plasma current at similar conditions. This approach allows for a more comprehensive understanding of the factors that influence plasma behavior and can provide valuable insights for future research in this area.

II. Experimental Setup

The study was conducted on the GOLEM tokamak at for different plasma current values to investigate the dependence of transport barrier formation on input power. This was achieved by incrementally changing the voltage on the current drive capacitor, starting at $300\ V$ and increasing in $50\ V$ steps up to $500\ V$, after which the step size was increased to $100\ V$ up to $800\ V$. Throughout all these scans, the pressure was maintained at a constant level. For each specific current drive voltage, radial profiles of electron temperature were measured using a combination of Ball-pen and Langmuir probes. Fast camera images were also generated to visually document the formation of transport barriers.

A. The GOLEM Tokamak

The GOLEM tokamak features a compact circular configuration, with a major radius of $0.4\ m$ and minor radius of $0.085\ m$, and operates with ohmic heating. It is also equipped with a limiter having a partial moon shape and made of molybdenum. It has a non-axisymmetric iron core for current drive. With a maximum plasma current of $5\ kA$ and toroidal magnetic field reaching up to $0.5\ T$, albeit non-constant during discharge, GOLEM provides a versatile experimental platform. Notably, this device lacks active gas puffing, resulting in uncontrolled plasma density, and typically achieves core electron temperatures around $100\ eV$ with line-averaged densities of up to $3 \times 10^{19}\ m^{-3}$. The experimental setup of GOLEM offers great reproducibility meaning that different shots with the same parameters yield similar results. Several different shots are shown in Figure 1 as a way to showcase the reproducibility of the relevant parameters for this study.

To facilitate plasma analysis, GOLEM is equipped with an array of diagnostic tools like magnetic coils, electric probes such as Langmuir and ball-pen probes, interferometers, spectroscopes, and fast cameras, all of which enable detailed measurements of plasma parameters. It is possible to achieve pre-ionization using a heated Tungsten wire. Another unique feature of GOLEM is its remote operation capabilities, which allow complete shot control. This includes control over plasma parameters and diagnostics which can be provided over the

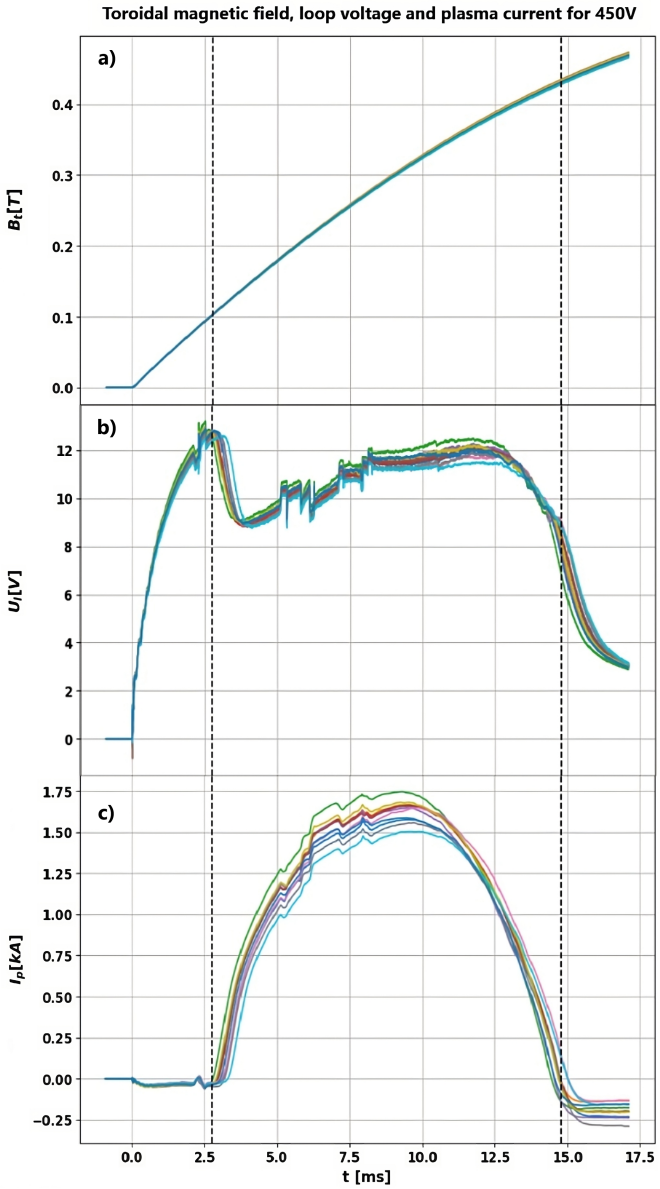

Fig. 1. Toroidal magnetic field (a), loop voltage (b), and plasma current (c) for 11 different shots at $U_{cd} = 450\ V$ for reproducibility. The vertical lines represent the begining and end of the plasma respectively.

web through a GUI. GOLEM also has access to various working gasses like H, D, He and Ar.

B. Diagnostic devices

This study focuses on measurements of the electron temperature, radial profiles (Figure 2), and electric fields using the combined Ball-pen and Langmuir probe system. The probe head is mounted on a motorized manipulator, enabling remote positioning and direct placement within the vacuum vessel using the discharge command.

The ball-pen probe is designed to balance the electron and ion saturation currents, making its floating potential equal to the plasma potential (ϕ). This is achieved by using a moving ceramic shield to screen off a portion of the electron current from the probe collector, taking advantage of the fact that electrons have a much smaller gyro-radius than ions in magnetized plasmas [2].

The Langmuir probe is used to determine the electron temperature, electron density, and floating potential (U_{fl}) of the plasma. It has different modes of operation for example by applying a constant or time-varying electric potential between the probe and the surrounding vessel to measure the Ion saturation current or IV characteristics to derive plasma properties. In our case, the probe was left floating. to measure the floating potential of the plasma.

III. Methodology

A. Data acquisition

Taking advantage of the consistent reproducibility achieved by the GOLEM tokamak, a shot-by-shot approach was adopted to study the plasma characteristics. Specifically, parameters such as pressure, toroidal magnetic field intensity, plasma current magnitude, and loop voltage amplitude were maintained at fixed values throughout a particular series of shots.

To minimize impurities within the chamber, GOLEM was subjected to an intensive glow-discharge-based cleaning routine followed by thermal baking processes. These procedures were implemented to minimize impurities that might otherwise compromise the overall integrity of the experiment.

More than a hundred distinct shots were executed across various operational configurations, further details are readily accessible through the official GOLEM tokomak shot database, with shot numbers between [47012-47137]. All discharges from our scans are marked as "He EMTRAIC probe scan" in the discharge comment [4].

The voltage of the current drive capacitor (U_{cd}) was progressively increased to study the conditions under different values of the plasma current, obtaining data for 300 V, 350 V, 400 V, 450 V, 500 V, 600 V, 700 V, and 800 V. Eleven shots were performed for each voltage, each for different radial position of the probes ranging from 42 mm from the plasma core all the way to 82 mm in intervals of 4 mm.

B. Data processing

All data was imported from the shot database using Python and several of its most well-known modules, notably Numpy and Xarray for numerical calculations, Pandas for importing and data management, Scipy and Scikit-learn for fitting, and Matplotlib for visualization. The entire analysis process was hosted on the Jupyterlab servers of the Institute for Plasma Physics (IPP).

The comprehensive dataset consists of different radial positions, each having thousands of points in time for a particular current drive voltage. These were used to reconstruct the radial profiles and the time evolution of the electron temperature gradient inside the transport barrier. To minimize potential errors and uncertainties, the dataset was truncated to exclude the plasma startup and shutdown phases, during which the plasma density was too low to provide accurate measurements.

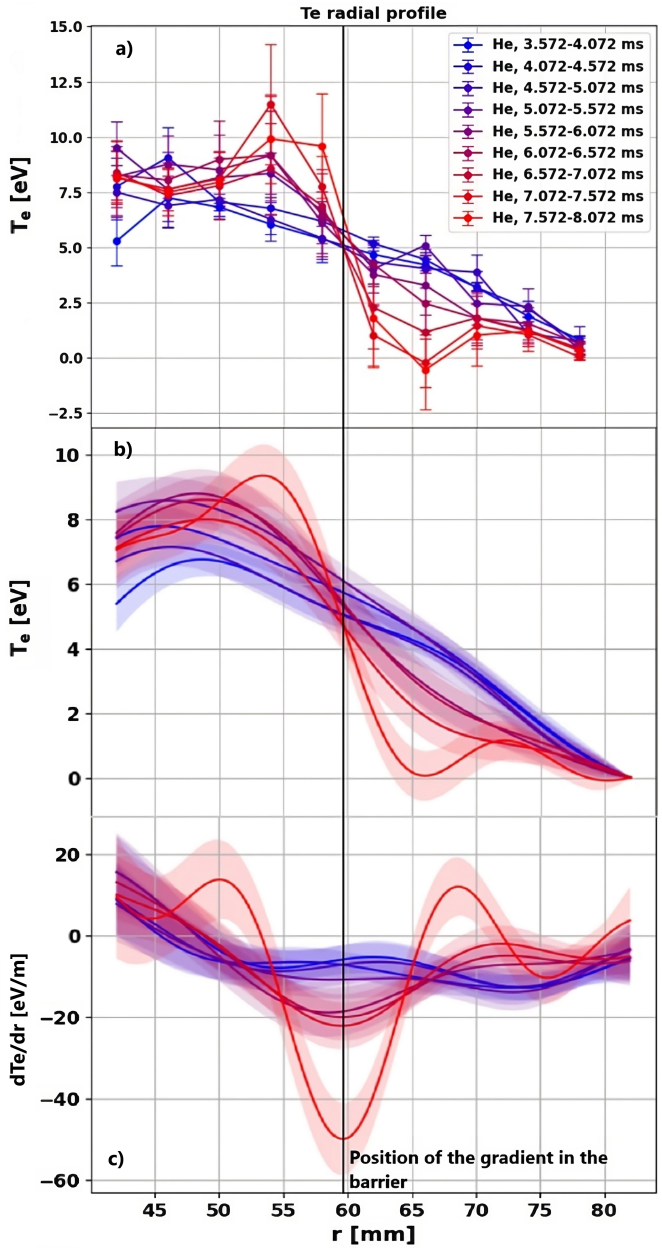

Fig. 2. Process of data analysis, starting with the raw data (a), then the Gaussian regression (b), and then the derivative with respect to the radial coordinate (c). Here, the lines are colormapped, with bluer lines corresponding to earlier time intervals and redder lines corresponding to later time intervals as shown in the legend for figure (a).

1) Calculation of the temperature: To find the temperature of the electrons at the location of the probe, Formula 1 was used. The calibration factor α and the expression itself were obtained from [5], where a more in-depth explanation of the calibration process can be found. The plasma potential was measured by the Ball-pen probe, and floating potential was measured by the Langmuir probe.

$$T_e[eV] = \frac{\Phi - U_{fl}}{\alpha}, \qquad \alpha[V/eV] = 2.0 \pm 0.2 \tag{1}$$

One important remark is that both the Langmuir probe and the Ball-pen probe are needed to find the electron temperature,

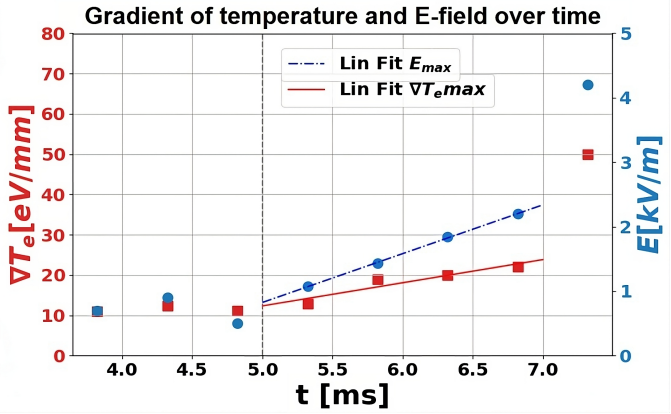

Fig. 3. Evolution of the temperature gradient and radial E-field for $U_{cd} = 450$ V with a linear fit after transition.

but they are not located in exactly the same position. This can lead to different measurements, particularly for very large gradients (such as the one found inside the transport barrier). This discrepancy can lead to negative temperature calculations, so a correction was put in place by interpolating the measurements and positions of the probes.

2) Calculation of the electric field: The calculation of the electric field is performed directly from the measurements of the plasma potential. The raw data was interpolated (as explained in Section III-B3) to increase the number of points for the calculation of the derivative, according to 2. The derivative is then performed using first order finite differences.

$$E_r[V/m] = -\frac{\partial \phi}{\partial r} \tag{2}$$

3) Binning and interpolation: Due to rapid plasma fluctuations, the data was binned into time intervals of 0.5 ms to perform a time average of these fluctuations. Average temperatures and electric field values, as well as their corresponding standard deviations, were calculated for each time interval (Figure 2.a). These points were then fitted using a Gaussian Process Regressor offered by Scikit [1] to increase the number of points in the radial direction (Figure 2.b). This increases the number of points for the calculation of derivatives, for temperature and potential, as previously explained (Figure 2.c).

4) Obtaining the results: The evolution of the temperature gradient inside the barrier and the electric field were monitored over time (as shown in Figure 3). A linear fit was made for an interval of 2 ms after transition for both the electric field and the temperature gradient for each current drive voltage. Furthermore, the maximum temperature gradient within this interval was used to derive the scaling laws.

IV. Results

A. Linear fit of the slopes

The slopes of the electric field and electron temperature gradient depicted in Figure 4 were compared after the transition. The results are plotted in Figure 4. The concurrent increase in both slopes suggests a strong correlation between them.

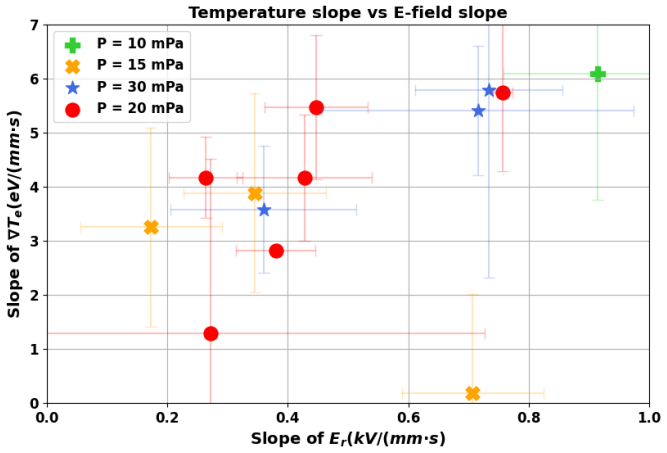

Fig. 4. Slope of the temperature gradient vs slope of the radial E-field (after the barrier formation).

There is a clear dependence between the two. Finding a corelation formula would be an interesting topic for future research, for which more data is required. On a more qualitative approach, this relationship is to be expected since an increased radial electric field results in higher poloidal velocity. This causes shearing which is directly related to the suppression of turbulence, hence the appearance of steep gradients in the temperature [3].

B. Scaling laws

To examine in more detail the evolution of the temperature gradient, the post-transition gradient was normalized using the pre-transition gradient, which was observed to be relatively constant in time, as shown in Figure 3. The normalized gradient was then plotted against the input power, revealing a dependence on power as expected and, interestingly, pressure. By including the pressure squared on the x-axis, a linear relationship was discovered between the normalized gradient and the product of input power and pressure squared (Figure 5). A linear fit was applied to this data to show a quantitative relationship between these parameters.

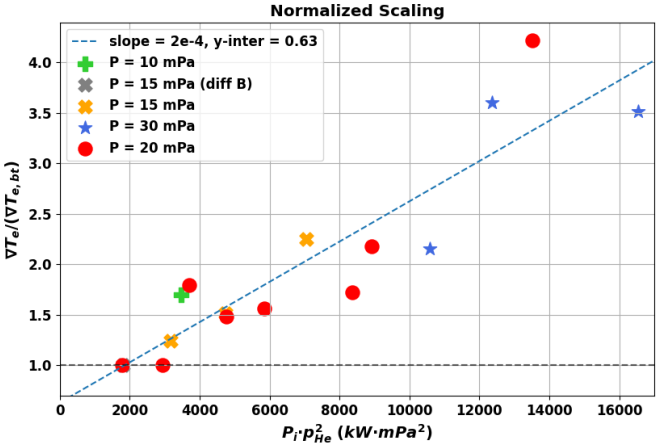

Fig. 5. Scaling law for the normalized temperature gradient.

V. Conclusions

This study presents our analysis of a spontaneously formed transport barrier, contributing to the understanding of transport barriers and their role in plasma confinement in the GOLEM tokamak. A distinctive feature of the transport barrier is the emergence of a sharp gradient in electron temperature within the scrape-off layer, accompanied by a gradually increasing electric field. The analysis process involved meticulously extracting and organizing data from the GOLEM diagnostics and combining it with existing datasets for processing. This comprehensive dataset enabled the creation of radial profiles for electron temperature and electric field, which, upon fitting, verify the presence of a transport barrier marked by a steep gradient in both temperature and electric field.

Our results show that an increase in the slope of the electron temperature gradient and the radial electric field occur simultaneously, even if the exact relation between them is yet to be discovered. Moreover, the electron temperature gradient exhibits a linear dependence on the input power and a quadratic dependence on the chamber pressure, as shown in Figure 5. This is the first approximation of this phenomenon, offering insight into the parametric dependence and dynamics of the transport barrier. These results will become relevant in future research in order to specifically target points of interest that can improve our understanding of the spontaneous formation of transport barriers in circular tokamaks.

Future studies could also include refining the current scaling laws to determine the key parameters and their precise relation with the formation of the transport barrier and exploring the impact of variable magnetic fields. Additionally, extending this study to hydrogen gas and using the current scaling laws on other devices with circular cross-section would provide a valuable point of comparison, helping further the understanding of the properties of transport barriers all the while making smaller devices relevant to fusion related studies again.

References

[1] *1.7. Gaussian Processes*. en. URL: https://scikit-learn/stable/modules/gaussian_process.html.

[2] L. Conde. "An introduction to Langmuir probe diagnostics of plasmas". In: 2011. URL: https://www.semanticscholar.org/paper/An-introduction-to-Langmuir-probe-diagnostics-of-Conde/38a25b48f657113123ed5f0579caa7a3bf50622f.

[3] "Effect of the radial electric field on turbulence". en. In: (). URL: https://inis.iaea.org/records/qq3wd-q7m61.

[4] *Golem #47012*. URL: http://golem.fjfi.cvut.cz/shots/47012/.

[5] P. Macha et al. "Spontaneous formation of a transport barrier in helium plasma in a tokamak with circular configuration". en. In: *Nuclear Fusion* 63.10 (Sept. 2023). Publisher: IOP Publishing, p. 104003. ISSN: 0029-5515. DOI: 10.1088/1741-4326/acf1af. URL: https://dx.doi.org/10.1088/1741-4326/acf1af.